IgG1 and IVIg induce inhibitory ITAM signaling through FcγRIII controlling inflammatory responses

Meryem Aloulou,[1,2] Sanae Ben Mkaddem,[1,2] Martine Biarnes-Pelicot,[1,2] Tarek Boussetta,[1,2] Hervé Souchet,[1,2] Elisabetta Rossato,[1,2] Marc Benhamou,[1,2] Bruno Crestani,[2-4] Zhou Zhu,[5] Ulrich Blank,[1,2] Pierre Launay,[1,2] and Renato C. Monteiro[1,2,6]

[1]Inserm U699, Paris, France; [2]Université Paris Diderot, Sorbonne Paris Cité, Inflamex Laboratory of Excellence, Faculté de Médecine, Site Xavier Bichat, Paris, France; [3]Inserm U700, Paris, France; [4]Service de Pneumologie, Assistance Publique–Hôpitaux de Paris, Hôpital Bichat, Paris, France; [5]Division of Allergy and Clinical Immunology, Johns Hopkins Asthma and Allergy Center, Baltimore, MD; and [6]Assistance Publique–Hôpitaux de Paris, Hôpital Bichat, Service d'Immunologie, Paris, France

Intravenous immunoglobulin (IVIg) has been used in the treatment of several autoimmune and inflammatory diseases. However, its mechanism of action remains incompletely understood. Here, we investigated the possibility that IVIg induces its anti-inflammatory effects through activating Fcγ receptors bearing an immunoreceptor tyrosine-based activation motif (ITAM) in the FcRγ signaling adaptor. Recently, the concept of inhibitory ITAM (ITAMi) has emerged as a new means to negatively control the immune response. We found that interaction of FcRγ-associated mouse or human FcγRIII with uncomplexed IgG1 or IVIg, or with bivalent anti-FcγRIII F(ab′)$_2$ reduced calcium responses, reactive oxygen species production, endocytosis, and phagocytosis, induced by heterologous activating receptors on monocyte/macrophages and FcγRIII$^+$ transfectants. Inhibition required the ITAMi configuration of the FcγRIII-associated FcRγ subunit and SHP-1 recruitment involving formation of intracellular "inhibisome" clusters containing FcγRIII, and the targeted heterologous activating receptor. IVIg as well as anti-FcγRIII treatments controlled the development of nonimmune mediated inflammation in vivo independently of FcγRIIB. These results demonstrate that circulating immunoglobulins (Ig)Gs are not functionally inert but act through continuous interaction with FcγRIII-inducing ITAMi signaling to maintain immune homeostasis. These data support a new mechanism of action for IVIg and demonstrate the therapeutic potential of FcγRIIIA targeting in inflammation. (*Blood*. 2012; 119(13):3084-3096)

Introduction

Intravenous immunoglobulin (IVIg) is used not only for treatment of immune deficiencies, but also constitutes a therapeutic option in a large number of autoimmune, allergic, and inflammatory diseases.[1,2] Different mechanisms have been suggested as responsible for the anti-inflammatory activity of IVIg such as, its content of natural polyreactive Abs reactive, its ability to stimulate or block cellular receptors for immunoglobulins (Igs; Fc receptors, or FcRs), inhibition of the complement cascade, modulation of cytokine production, neutralization of auto-antibodies, and differential antibody glycosylation.[1,3-6]

FcγR exist in multiple isoforms comprising high-affinity and low-affinity receptors. In humans, there is one high-affinity IgG receptor, FcγRI (CD64), and 2 families of low-affinity IgG receptors, FcγRIIA, IIB, and IIC (CD32), and FcγRIIIA and IIIB (CD16). FcγRI and FcγRIIIA are associated with the common signaling adaptor FcRγ, whereas FcγRIIA, FcγRIIB and FcγRIIC are single-chain receptors and FcγRIIIB is a glycosyl-phosphatidyl inositol (GPI)–anchored receptor. In mice, there is no homolog to FcγRIIA and FcγRIIIB, but they express another FcRγ-associated receptor, the FcγRIV, that is not found in humans.[7] The FcRγ chain contains a tyrosine-based activation motif (ITAM) and is the prime effector of the proinflammatory activity of IgG in inflammatory and autoimmune diseases. Cross-linking of activating FcγRs, such as FcγRI, FcγRIII and FcγRIV, by immune complexes, launches transmembrane signaling after phosphorylation of ITAM tyrosine residues in the receptor-associated FcRγ subunit by kinases of the Src family.[8,9] For example, FcγRIII multimerization exacerbates inflammation in several models of immune complex-mediated diseases.[10-12] By contrast, FcγRIIB, which is conserved in mice and humans, is a single-chain inhibitory FcγR. FcγRIIB contains tyrosine-based inhibition motif (ITIM) in its cytoplasmic region.[13] Inhibition was shown to depend on the isotype of IgG and on FcγRIIB expression levels. Up-regulation of the latter was proposed as one of the mechanisms for the anti-inflammatory action of IVIg therapy.[1] FcγR anti-inflammatory activities of IVIg are mediated through both FcγRIIB- and/or FcγRIIIA-dependent and FcγR-independent mechanisms.[14-16] However, mechanisms of action of IVIg through activating FcγRIII are not yet fully elucidated.

The classic concept of the functional polarity of ITIM and ITAM motifs has been recently reevaluated. Several studies have demonstrated that ITAM can also initiate inhibitory signaling toward heterologous receptors.[17-19] This active inhibitory signaling by ITAM-bearing receptors was named inhibitory ITAM (ITAMi).[18] Thus, the FcαRI that is associated with the ITAM-bearing adaptor FcRγ, was found to act as a bifunctional module which, depending on the type of interaction with its ligand, induces either activating

Submitted August 25, 2011; accepted February 6, 2012. Prepublished online as *Blood* First Edition paper, February14, 2012; DOI 10.1182/blood-2011-08-376046.

The online version of this article contains a data supplement.

The publication costs of this article were defrayed in part by page charge payment. Therefore, and solely to indicate this fact, this article is hereby marked "advertisement" in accordance with 18 USC section 1734.

or inhibitory cell signaling. Although multivalent cross-linking of FcαRI with IgA-immune complexes induced proinflammatory signaling, monovalent FcαRI targeting with IgA in the absence of antigen can trigger inhibitory signals toward a whole array of cellular functions such as IgG-dependent phagocytosis, IgE-dependent degranulation, and TLR- or cytokine-mediated responses.[20,21] Strikingly, monomeric IgA binding induces weak ITAM-phosphorylation, transient recruitment of Syk followed by stable recruitment of SHP-1, whereas multivalent aggregation promotes strong ITAM phosphorylation with stable Syk recruitment. Recruitment of SHP-1 in the ITAMi configuration promotes the actin depolymerization-dependent "trapping" of FcαRI and of the targeted activating receptors within the same lipid rafts, which is followed by the appearance of intracellular inhibisome clusters.[22] Recently, FcγRIII, on direct interaction with *Escherichia coli*, was shown to launch an FcRγ-dependent inhibitory pathway that down-regulates MARCO scavenger receptor signaling, thereby preventing *E coli* phagocytosis.[23]

Based on these observations we hypothesized that the interaction between FcRγ-associated FcγRIII and its natural ligand IgG1 and IVIg might not be a passive event but could induce ITAMi signaling. Therefore, we investigated whether FcγRIII targeting with a specific antibody or its natural ligand IgG might induce anti-inflammatory activity through ITAMi signaling. Our results show that such targeting induces a potent and long lasting ITAMi inhibitory signal that operates through murine as well as human FcγRIII-FcRγ both in vitro and in vivo, revealing a previously unsuspected function of free IgG and IVIg, which is to dampen inflammatory responses and contribute to the regulation of tissue homeostasis.

Methods

Mice

BALB/c *FcγRIIB*$^{-/-}$ mice[24] were obtained from Taconics. BALB/c *FcγRIIB*$^{-/-}$ mice[10,25] were kindly provided by S. Verbeek (Leiden University, The Netherlands). Homozygous viable motheaten (*Ptpn6*$^{me-v}$) mice (*mev/mev*) on C57BL/6 genetic background were generated as described.[26] Briefly, heterozygous viable motheaten (*Ptpn6*$^{me-v}$) mice (*mev/+*) on C57BL/6 genetic background purchased from The Jackson Laboratory), were interbred to generate homozygous *mev/mev* mice which are deficient in SHP-1.[27] The genotype of the mice was determined following the protocols provided by The Jackson Laboratory.

Cell culture and reagents

Bone marrow–derived macrophages (BMMs) from 6- to 8-week-old mice were prepared. BMMs were obtained after a 7-day culture of bone marrow (BM) cells with colony-stimulating factor (CSF)–1.[28] RBL-2H3 mast cells expressing FcγRIII-FcRγ chimeras were maintained in Dulbecco modified Eagle medium (DMEM) supplemented with 10% fetal calf serum (FCS) and 1 mg/mL G418 (Invitrogen). Human macrophages were obtained by bronchoscopy from healthy nonsmoking subjects at Bichat hospital with their informed consent in accordance with the Declaration of Helsinki and approved by the Bichat Ethical committee. Human peripheral blood mononuclear cells (PBMCs) were isolated from healthy volunteers by Ficoll-Hypaque density gradient centrifugation. [24,25]All experiments were performed in accordance with the Bichat Animal Facility guidelines and were approved by the Bichat Ethical committee. Rat anti–mouse (2.4G2) FcγRII/III,[29] mouse anti–human FcγRIII (3G8),[30] and irrelevant control mAbs were used as $F(ab)'_2$ and Fab fragments. $F(ab)'_2$ and Fab were prepared as described.[20,31] Mouse anti-DNP–specific IgE (H1-ϵ-26.82) was obtained as described.[32] Mouse monoclonal IgG1 was purified from hybridoma clone A62 as described.[20,33] IVIg (Privigen; 100 mg/mL) was purchased from CSL Behring Gmbh.

Endocytosis and phagocytosis assays

For endocytosis, 5×10^5 BMMs were allowed to adhere on chamber slides (Lab-tek 8 wells, Nalge Nunc International) and treated with lipopolysaccharide (LPS; 100 ng/mL) during 12 hours to induce MARCO expression.[34] Cells were washed and incubated with indicated FcγRIII targeting reagents and in some instances with goat anti–rat $F(ab')_2$. After washing, Acetylated low-density lipoprotein (acLDL) endocytosis was induced by adding Alexa fluor 488–coupled acLDL (10 μg/mL) for 30 minutes at 37°C. Cell surface was decorated by staining with biotinylated antibody to mouse CD11b (M1/70, Serotec) on ice for 20 minutes plus streptavidin–Alexa 568. To block acLDL endocytosis, cells were preincubated with 10 μg/mL of anti-MARCO rat mAb ED31 (Serotec) for 30 minutes at 37°C. For phagocytosis, cells were allowed to adhere 8-well-chamber slides at 5×10^5 cells per well for 12 hours and nonadherent cells were removed. Adherent cells were incubated with candidate $F(ab')_2$ (10 μg/mL). Phagocytosis was initiated by incubation of Alexa Fluor 594–labeled *Staphylococcus aureus* (5×10^5 per 10^6 bacteria; Molecular Probes) for 30 minutes at 37°C. Slides were mounted and examined with a confocal laser microscope (LSM 510 Carl Zeiss).

Measurement of ROS production

Blood human monocytes or neutrophils (5×10^5) were purified from healthy donors and resuspended in 0.5 mL Hanks balanced salt solution (HBSS) containing 10μM luminol (Sigma-Aldrich) with 3G8 $F(ab')_2$ at 5 to 10 μg/mL or irrelevant 320 $F(ab')_2$ at 10 μg/mL for 20 minutes. Cells were stimulated with 10^{-6}M of N-formyl-methionine-leucine-phenylalanine (fMLF; Sigma-Aldrich). Chemiluminescence was recorded with a luminometer (Berthold-Biolumat LB937).

cDNA constructs, expression vectors, and transfection

The human FcγRIIIA sequence was amplified from plasmid pWX-puro FcγRIII LL 649 kindly provided by Dr L. Lanier (University of California, San Francisco). The FcγRIIIA-FcRγ chimera was generated as follow. The extracellular domain of the human FcγRIII (F: TAG**TCTAGA**TGGTGGTGCAAATCAAAGAAC and R: GGCATCCAGGATATAGCAGAGTGGAAAGAATGATGAGATGGTTG) as well as the transmembrane and intracellular domain of the human FcRγ chain (F: CAACCATCTCATCATTCTTTCCACTCTGCTATATCCTGGATGCC and R: TAG**GGATCC**CTACTGTGGTGGTTTCTCATG) were amplified by PCR. Products were fused by overlapping PCR. FcγRIIIA-FcRγ chimeric sequences were cloned into *Xba*I-*Bam*HI restriction sites (primers in bold) of pBJ1neo plasmid, derived from pcDL-SRα-296, containing the SRα promoter. Point mutations (Y246F, Y257F, and Y246-257F) were introduced in the ITAM motif of the FcγRIIIA-FcRγ chimera using Stratagene QuikChange site-directed mutagenesis kit. All constructs were verified by sequencing before transfection into RBL-2H3 cells by electroporation. Stable G418 resistant clones were selected, and FcγRIIIA expression levels and exocytosis capacity were determined.

β-hexosaminidase assay

Exocytosis was determined by measuring release of the granule enzyme β-hexosaminidase as described.[35] Briefly, cells were sensitized overnight at 37°C with IgE anti-DNP (5 μg/mL) and reagents were added as indicated in the figure legends. Exocytosis was induced by 0.1 μg/mL DNP-HSA antigen (Sigma-Aldrich) at 37°C for 45 minutes. In some experiments, cells were directly incubated with candidate $F(ab)'_2$ (10 μg/mL) on ice and degranulation was triggered at 37°C by addition of rabbit anti–mouse $F(ab')_2$ (RAM at 40 μg/mL) for 45 minutes.

Immunoprecipitation and immunoblotting

Cells were solubilized in 1% digitonin-containing lysis buffer[20] and FcγRIII were immunoprecipitated for 2 hours at 4°C with either protein G

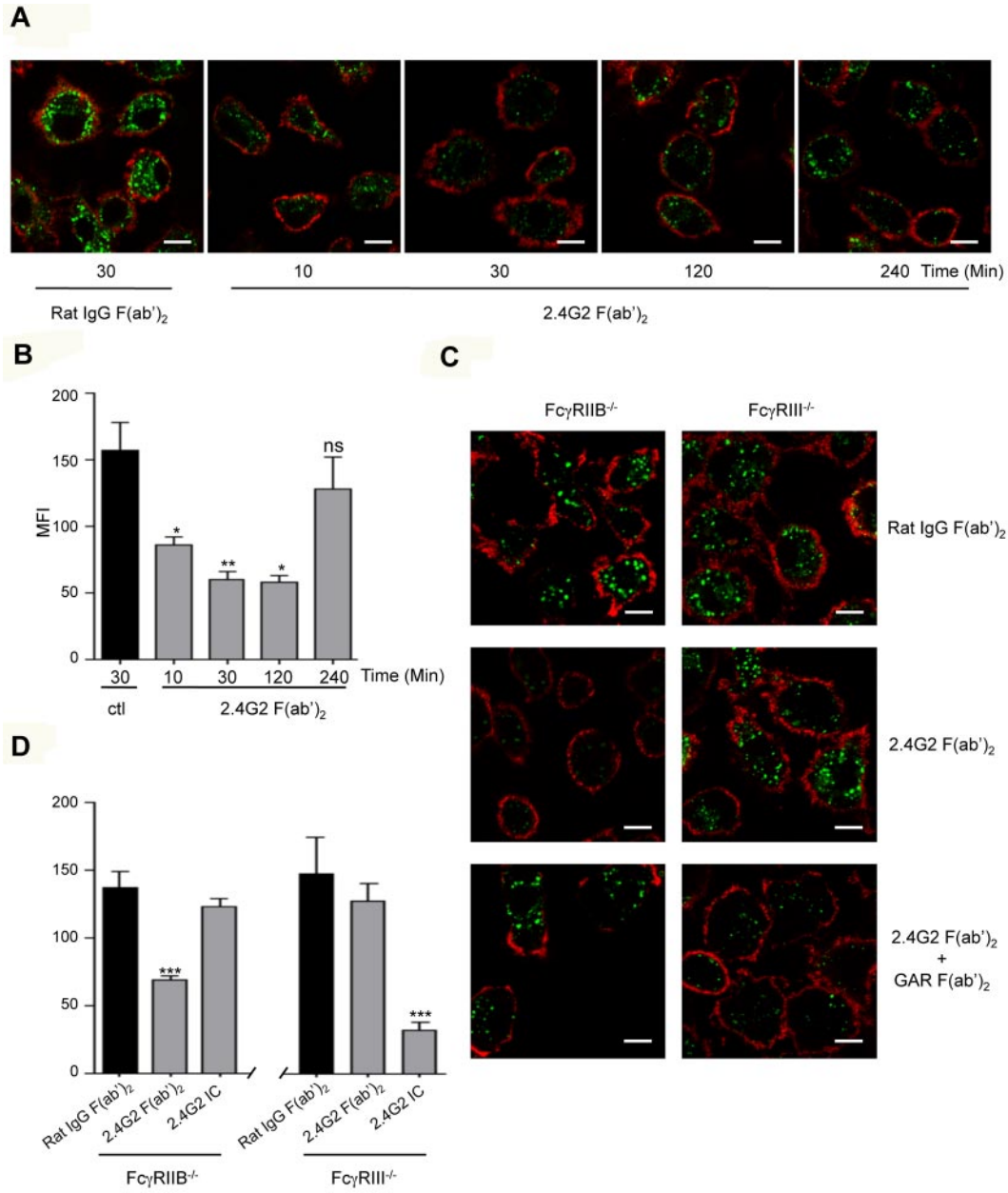

Figure 1. Bivalent crosslinking of mouse FcγRIII inhibits acLDL endocytosis. (A) Cultured BMM (5×10^5/well) derived from *FcγRIIB*$^{-/-}$ mice were treated with lipopolysaccharide (LPS; 100 ng/mL) for 12 hours to induce MARCO expression. Cells were preincubated with 2.4G2 F(ab′)$_2$ anti-FcγRII/III (10 μg/mL) or irrelevant rat IgG F(ab′)$_2$ for the indicated times at 37°C, followed by incubation with Alexa Fluor 488–coupled acLDL for 30 minutes to allow endocytosis. Cells were then stained with CD11b-biotin and streptavidin-Alexa 568 on ice for 20 minutes to delineate the cell surface before confocal microscopy. Scale bars: 5 μm. (C) LPS-primed BMMs from *FcγRIIB*$^{-/-}$ or *FcγRIII*$^{-/-}$ were treated with irrelevant rat IgG F(ab′)$_2$ (10 μg/mL) or with 2.4G2 F(ab′)$_2$ (10 μg/mL) alone or 2.4G2 F(ab′)$_2$ plus goat anti–rat F(ab′)$_2$ (GAR at 40μg/mL) for 30 minutes at 37°C and acLDL endocytosis was induced as before. Representative merged optical sections are presented showing internalized acDL inside the cells. Scale bars: 5 μm. (B-D) Quantitative analysis of acLDL endocytosis experiments performed in panels A and C, respectively. Green mean fluorescence intensity (MFI) inside each cell was quantified using LSM510 analysis software that analyzes specific pixels in at least 5 confocal microscope fields (*$P < .05$, **$P < .01$, ***$P < .001$; n = 5; nonparametric Mann-Whitney test).

or 3G8 F(ab′)$_2$ coupled to CNBr-activated sepharose 4B (Amersham-Pharmacia). Proteins were resolved by sodium dodecyl sulfate (SDS)–10% polyacrylamide gel electrophoresis (PAGE), transferred onto nitrocellulose membranes (Invitrogen) and immunoblotted with primary antibodies such as rabbit anti–SHP-1 (Biotrend), rabbit anti-Syk (Santa Cruz Biotechnology), rabbit anti-phospho–Erk MAPK (Cell Signaling Technology), rabbit anti-Erk (Santa Cruz Biotechnology), and rabbit anti-phospho–SHP1 (ECM Biosciences) followed by goat anti–rabbit IgG (Jackson ImmunoResearch Laboratories) coupled to horseradish peroxidase (HRP). Membranes were developed by enhanced chemical luminescence (ECL) treatment (Amersham Biosciences).

Single cell calcium measurement

Cells were loaded with Fura2-AM in glass-bottom microwell dishes with 1μM of Fura2-AM and pluronic acid (both from Invitrogen) and incubated at 37°C during 30 minutes. Cells were then washed with Ringer solution (in mM: 145 NaCl, 5.4 KCl, 2 CaCl2, 1 MgCl2, 10 glucose, 10 N-(hydroxyethyl)piperazine-N′-2-ethanesulfonic acid (HEPES) and 0.1% BSA, pH 7.5 with NaOH), or in some instances, in 5mM ethylene glycobis(b-aminoethyl ester)–N,N,N′,N′-tetraacetic acid (EGTA) solution (Ringer solution without calcium and buffered with 5mM EGTA). Cells were excited by wavelengths of 340 and 380 nm. Fluorescence emission of several cells was simultaneously recorded at a frequency of 1 Hz using a dual excitation

fluorometric imaging system (TILL-Photonics) controlled by TILL-Vision Version 4.0 software. Signals from approximately 30 cells were computed into relative ratio units of the fluorescence intensity of the different wavelengths (340/380 nm).

Inhibisome formation

Cells were allowed to adhere in 8-well-chamber slides for 12 hours at 37°C. Cells were sensitized for 1 hour with Alexa Fluor 488–conjugated anti-DNP IgE (5 μg/mL) and incubated for 30 minutes with biotinylated 3G8 anti-FcγRIII F(ab)′$_2$ (10 μg/mL) before the addition of DNP-HSA for 10 minutes. Cells were successively fixed (with 3% paraformaldehyde), permeabilized (with 0.025% saponin), and saturated nonspecific sites, before incubation with rabbit anti–SHP-1 polyclonal antibodies (Santa Cruz Biotechnology) and the relevant secondary antibodies (cross-adsorbed anti–rabbit Alexa Fluor 647–conjugated goat antibody, and Alexa Fluor 568–conjugated steptavidin; Molecular Probes). Cells were mounted and examined with a confocal laser microscope (LSM 510 Carl Zeiss). Data were analyzed with LSM 510 image examiner software (W. Rasband, National Institutes of Health).

Flow cytometry

Cells were preincubated or not with 100 μg human IgG to block FcγRs before incubation with biotinylated anti–human FcγRIII 3G8 or irrelevant mAb plus streptavidin (SA)–PE (Sourthern Biotech Associates). After washing, cells were analyzed by FACScalibur flow cytometer and FlowJo Version 7.6.3 software (BD Biosciences).

Unilateral ureteral obstruction nephritis model

Nephritis was induced by unilateral ureteral obstruction (UUO) as described.[36] Animals were injected intraperitoneally with 100 μg/20 g body weight of 2.4G2 F(ab)′$_2$ or of rat IgG F(ab)′$_2$, or with 40 mg/20 g body weight of IVIg or of BSA, for 8 days at 48-hour intervals. The first dose was administered 24 hours before UUO. On day 8, animals were killed and kidneys were analyzed.

Immunohistochemistry

Acetone-fixed frozen kidney sections (3 to 4-μm-thick) were incubated with biotinylated rat anti–mouse mAb CD11b (BD Pharmingen) as described.[37] Infiltrating CD11b+ cells were counted blind under a microscope (Leica Microsystems) using a 40× objective. A minimum of 30 high-power fields (HPFs) were analyzed and data are expressed as cells/HPF.

Quantitative real-time PCR analysis

Kidneys were homogenized and RNA was prepared. RNA (100 ng) was reverse-transcribed using SuperScript III reverse transcriptase (Invitrogen). Resulting cDNA was used as template for qPCR analysis. Primers were purchased from Eurofins and were as follows: GAPDH: 5′-ACGGCAAATTCAACGGCACAGTCA-3′ (sense), 5′-TGGGGGCATCGGCAGAAGG-3′ (antisense); MCP-1: 5′-ATGCTTCTGGGCCTGCTGTTC-3′(sense), 5′-CTGCTGCTGGTGATCCTCTTGTAG-3′ (antisense); TNFα: 5′-AGGCACTCCCCCAAAAGATG-3′ (sense), 5′-TCACCCCGAAGTTCAGTAGACAGA-3′ (antisense). Gene quantification was performed in duplicate on Chromo4 Real-Time PCR Detection System (Biorad). Data were normalized to GAPDH values.

Results

Identification of mouse FcγRIII as an inhibitory receptor after IgG1 and IVIg binding

As IgG binds to several FcγRs, we first addressed whether specific targeting of mouse FcγRIII using an anti-FcγRII/III (2.4G2) antibody could inhibit MARCO-mediated endocytosis by BMMs. To exclude effects of ITIM-bearing FcγRIIB, which is also recognized by 2.4G2, BMMs from FcγRIIB-deficient mice (*FcγRIIB*$^{-/-}$) were used. acLDL is a known ligand of the scavenger receptor MARCO.[38] Neither expression of MARCO nor MARCO's ability to promote acLDL endocytosis were altered by the absence of FcγRIIB or of FcγRIII on BMM (supplemental Figure 1, available on the *Blood* Web site; see the Supplemental Materials link at the top of the online article). Preincubation of BMMs from *FcγRIIB*$^{-/-}$ mice with 2.4G2 F(ab′)$_2$ for 10 minutes to 2 hours inhibited acLDL endocytosis compared with irrelevant F(ab′)$_2$ fragments (Figure 1A-B). The inhibition of endocytosis occurred in a time-dependent manner reaching the maximal level at 30 minutes preincubation with the antibody. F(ab′)$_2$-mediated inhibition (2.4G2) was abolished in *FcγRIII*$^{-/-}$ BMMs (Figure 1-D) confirming that FcγRIII was the receptor that mediated this inhibitory signal. Inhibition was not observed with 2.4G2 Fab, instead of F(ab′)$_2$, fragments (supplemental Figure 2), which indicates that at least for 2.4G2, antibody-mediated inhibition might occur only when FcγRIII is dimerized. In contrast, further crosslinking of FcγRIII on *FcγRIIB*$^{-/-}$ BMMs failed to induce inhibition (Figure 1C-D), which indicates that, as for FcαRI, ITAMi function cannot be activated when receptors are extensively aggregated. In agreement with data showing that FcγRIIB can inhibit BCR signaling without coligation,[39] multimerization of ITIM-bearing FcγRIIB in *FcγRIII*$^{-/-}$ BMMs by 2.4G2 F(ab′)$_2$ plus goat anti–rat F(ab′)$_2$ inhibited acLDL endocytosis without coligation between FcγRIIB and MARCO. These results underscored that ITIM- and ITAM-bearing receptors mediate inhibition through different pathways.

To explore whether natural ligands of mouse FcγRIII are able to mediate inhibitory signaling, we evaluated endocytosis of acLDL by BMMs from either *FcγRIIB*$^{-/-}$ or *FcγRIII*$^{-/-}$ mice in the presence of a monomeric fraction of a mouse monoclonal IgG1. Monomeric IgG1 inhibited acLDL endocytosis in *FcγRIIB*$^{-/-}$ BMMs and this inhibition was abolished in the absence of FcγRIII (Figure 2A-B). This inhibition was dose dependent, reaching a significant effect at 10 mg/mL IgG1 (Figure 2). It was not observed in cells expressing FcγRIIB in the absence of FcγRIII even at IgG1 concentrations similar to those found in serum (Figure 2B). These experiments allowed us to conclude that only high concentrations of monomeric IgG1, which resemble polyclonal IgG1 concentrations in the plasma, can trigger an FcγRIII-dependent inhibitory pathway. The fact that inhibition was fully abolished in *FcγRIII*$^{-/-}$ BMMs excludes other Fcγ receptors, such as FcγRI and FcγRIV, as molecular targets of IgG1-inhibitory signals.

As monomeric monoclonal mouse IgG1 mediated inhibition through FcγRIII, we next investigated whether IVIg, which contain mainly IgG1, can similarly induce an inhibitory signal via FcγRIII. Preincubation of *FcγRIIB*$^{-/-}$, but not *FcγRIII*$^{-/-}$, BMMs with high concentrations of IVIg significantly inhibited acLDL endocytosis whereas irrelevant control BSA had no effect (Figure 3A, supplemental Figure 3). Likewise, direct targeting of FcγRIII on these cells by 2.4G2 F(ab′)$_2$, but not its extensive aggregation by 2.4G2 F(ab′)$_2$ immune complexes, inhibited acLDL endocytosis (Figure 3A, supplemental Figure 3). As IVIg can form multimeric species with donor or host IgG including mainly so called IgG dimers,[40] HPLC-purified fractions containing mononeric (IVmIg), or dimeric (IVdIg) IVIg (supplemental Figure 4) were prepared to address their effect on the blockade of acLDL endocytosis in *FcγRIIB*$^{-/-}$ BMMs (Figure 3B). These experiments indicated that polyclonal human

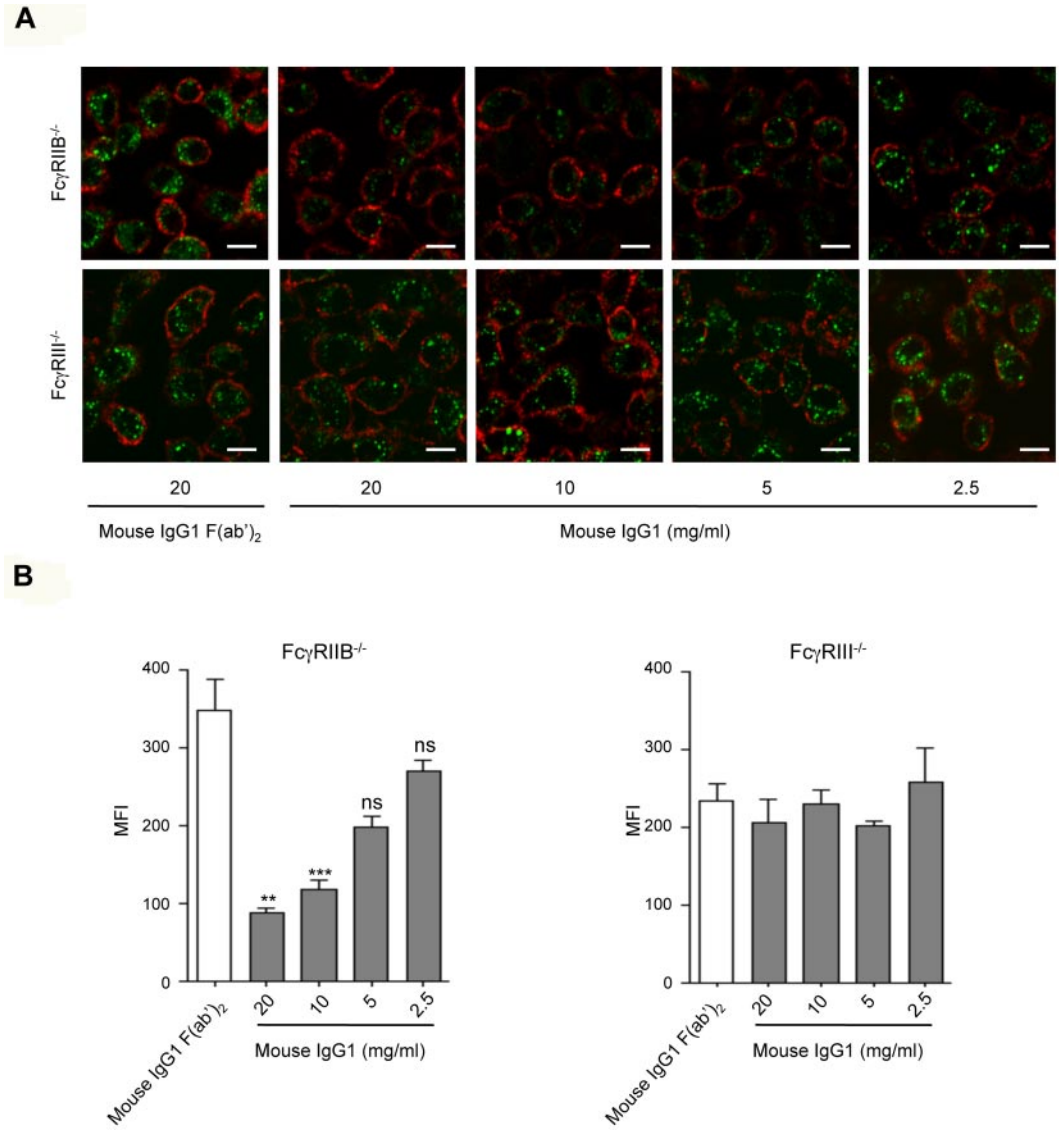

Figure 2. Monomeric mouse IgG1 inhibits acLDL endocytosis through FcγRIII. (A) LPS-primed BMMs (5×10^5/well) derived from *FcγRIIB*$^{-/-}$ or *FcγRIII*$^{-/-}$ mice were preincubated with mouse IgG1 or mouse IgG F(ab′)$_2$ at the indicated concentrations at 37°C for 30 minutes, followed by incubation with Alexa Fluor 488–coupled acLDL to allow endocytosis. Cells were then stained with CD11b-biotin and streptavidin–Alexa 568 on ice for 20 minutes to delineate the cell surface before endocytosis examination by confocal microscopy. Endocytosis was measured using confocal microscopy. Representative merged optical sections are presented showing internalized acLDL inside the cell. Scale bars: 5 μm. (B) Quantitative analysis of acLDL endocytosis experiments performed in panel A. Green MFI inside each cell was quantified using LSM510 analysis software that analyzes specific pixels in at least 5 confocal microscope fields (*$P < .05$, **$P < .01$, ***$P < .001$; n = 5; nonparametric Mann-Whitney test).

monomeric and dimeric IgG interacted with mouse FcγRIII and induced an inhibitory signal for endocytosis.

Inhibitory function of human FcγRIIIA is mediated by the FcRγ ITAM

Both mouse FcγRIII and its human homolog, the FcγRIIIA, are associated with the ITAM-bearing adaptor FcRγ.[7] Therefore, we next assessed whether human FcγRIIIA was also able to induce inhibition after specific targeting by F(ab′)$_2$ anti–human FcγRIII (3G8). Preincubation of human alveolar macrophages, which express both FcγRIIIA and MARCO (supplemental Figure 5), with 3G8 F(ab′)$_2$ inhibited MARCO-mediated phagocytosis of *S aureus* (Figure 4A).

Because monocytes express FcRγ-associated FcγRIIIA, whereas neutrophils express the signaling incompetent GPI-anchored FcγRIIIB,[41] we next examined FcγRIII-inhibitory signaling in both cell types. The formylated peptide f-Met-Leu-Phe (fMLF), derived from bacteria, was used as a stimulus as it induces ROS production in both monocytes[42] and neutrophils.[43] Preincubation of monocytes with 3G8 F(ab′)$_2$ inhibited fMLF-mediated ROS production in a dose-dependent manner whereas irrelevant F(ab′)$_2$ had no effect (Figure 4B). By contrast, preincubation of human neutrophils with 3G8 F(ab′)$_2$ failed to inhibit response to fMLF (Figure 4C), which indicates that inhibition required the FcγRIIIA-associated FcRγ signaling adaptor.

To demonstrate whether the inhibitory function involves an ITAMi-mediated mechanism,[18] wild-type (WT) and mutant FcγRIII-FcRγ chimera were generated (Figure 5A top panel) and transfected into the rat mast cell line RBL-2H3 yielding significant level of expression at the cell surface (Figure 5A bottom panels). As RBL-2H3 mast cells express FcεRI, we evaluated inhibition by the transfected chimeric receptors of IgE-dependent exocytosis. Preincubation of WT transfectants with anti–human FcγRIII 3G8 F(ab′)$_2$, but not with irrelevant 320 F(ab′)$_2$, markedly inhibited

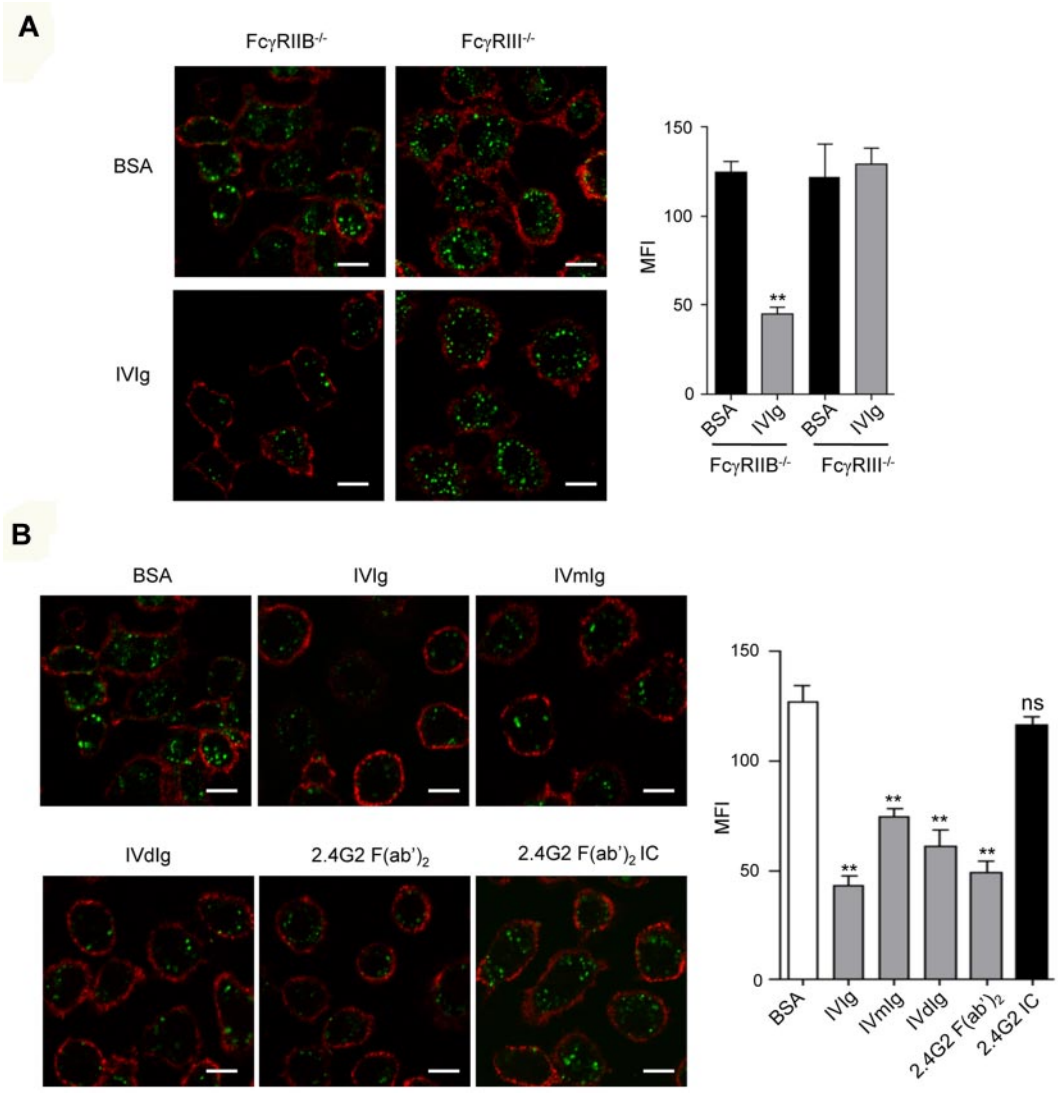

Figure 3. Human IVIg inhibits acLDL endocytosis through FcγRIII. (A) LPS-primed BMM from *FcγRIIB*$^{-/-}$ or *FcγRIII*$^{-/-}$ mice were incubated with IVIg (18 mg/mL) or with BSA (18 mg/mL) for 30 minutes at 37°C. Alexa Fluor 488–coupled acLDL was added to allow endocytosis for 30 minutes followed by plasma membrane staining using anti-CD11b–biotin and streptavidin–Alexa 568 before confocal analyses. Left panels show representative merged optical sections of internalized acDL inside the cell. Scale bars: 5 μm. Right panel indicates quantification of acLDL endocytosis using green MFI inside each cell as quantified by LSM510 analysis software that analyzes specific pixels in at least 5 confocal microscope fields (**$P < .01$; nonparametric Mann-Whitney test). (B) LPS-primed BMMs from *FcγRIIB*$^{-/-}$ mice were preincubated with 10 mg/mL unfractionnated IVIg, with HPLC-purified monomeric (IVmIg) or HPLC-purified dimeric IVIg (IVdIg) or BSA as a control. Cells were also preincubated with 10 μg/mL of 2.4G2 F(ab′)$_2$ or immune complexes (IC) made of 2.4G2 F(ab′)$_2$ (10 μg/mL) plus goat anti–rat F(ab′)$_2$ (GAR at 40μg/mL) for 30 minutes at 37°C. Endocytosis was induced by addition of Alexa Fluor 488–coupled acLDL. The plasma membrane was stained with CD11b-biotin and streptavidin–Alexa 568 on ice for 20 minutes and cells were analyzed using confocal microscopy. Representative merged optical sections are presented showing internalized acDL inside the cell. Scale bars: 5 μm. Green mean fluorescence intensity (MFI) inside each cell was quantified (right panel) using LSM510 image examiner software that analyzes specific pixels in at least 5 confocal microscope fields (**$P < .01$; n = 5; nonparametric Mann-Whitney test).

IgE-dependent cell degranulation (Figure 5B). This effect was abolished in double, as well as single, Y-to-F FcRγ ITAM mutant transfectants, which shows that both tyrosine residues are involved in the inhibitory process. Furthermore, multimeric crosslinking could induce FcγRIII-mediated exocytosis in WT but not in mutant transfectants RBL-2H3 cells (Figure 5C). These results indicate that, similar to the activating response, the inhibitory responses through FcγRIIIA are ITAM-dependent. We next evaluated whether human polyclonal IgG (IVIg preparations) could also inhibit mast cell exocytosis in transfectants expressing the FcγRIIIA-FcRγ chimera. Figure 5D shows that, as previously described, only high concentrations of IVIg (> 5 mg/mL) were able to inhibit FcεRI degranulation. Morever, FcγRIII-FcRγ chimera-mediated IVIg action required 2 hours to be optimal, whereas inhibition mediated by 3G8 F(ab′)$_2$ anti-FcγRIII was already maximal at 30 minutes. This suggests that besides the degree of aggregation of the FcγRIII ligands, their affinity for the receptor ligand is another important parameter that controls the inhibitory function of FcγRIII.

Analysis of ITAMi inhibitory signaling by FcγRIIIA

We have shown previously that ITAMi signaling via FcαRI involves a series of specific signaling responses that explain the ITAMi-mediated inhibitory actions. To identify whether IgG or antibody-mediated targeting of FcγRIII induced similar inhibitory signaling, we used RBL-2H3 transfectants expressing FcγRIII-FcRγ chimera. Figure 6A shows that preincubation with either IVIg or 3G8 F(ab′)$_2$, but not irrelevant 320 F(ab′)$_2$ (supplemental Figure 6), induced a transient recruitment (up to 30 minutes) of Syk to the chimera, which was followed by stable recruitment (at least

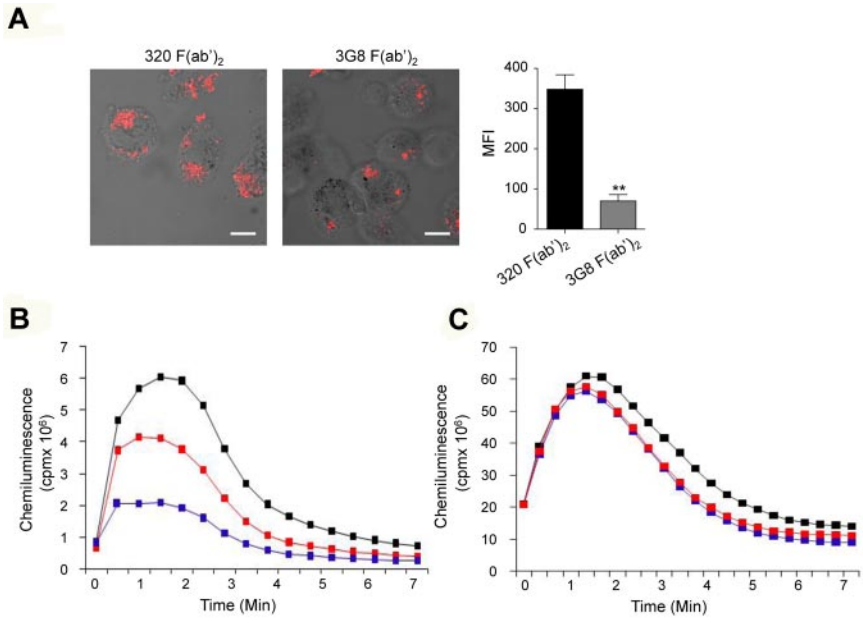

Figure 4. Bivalent crosslinking of human monocyte/macrophage-expressed FcγRIIIA but not neutrophil-expressed FcγRIIIB inhibits bacterial phagocytosis and ROS production. (A) Human alveolar macrophages (5×10^5) were allowed to adhere on glass cover slips for 12 hours at 37°C followed by preincubation with 10 μg/mL anti–human FcγRIII F(ab′)$_2$ (3G8) or irrelevant F(ab′)$_2$ (320) for 30 minutes at 37°C. Phagocytosis assay was initiated by addition of alexa fluor 594-coupled *S aureus* for 30 minutes at 37°C and evaluated by confocal microscopy. Representative merged optical sections are presented showing internalized *S aureus* inside the cell. Scale bars: 5 μm. Internalized *S aureus* were quantified by determining red MFI inside each cell using LSM510 image analysis software (**$P < .01$; n = 3; nonparametric Mann-Whitney test). (B) Human blood monocytes (5×10^5 cells/0.5 mL Hanks buffer) were preincubated with the indicated concentration of 3G8 F(ab′)$_2$ or 10 μg/mL of irrelevant 320 F(ab′)$_2$ for 30 minutes at 37°C before cell activation with fLMF (10^{-6}M), and luminol-amplified chemiluminescence was measured. (C) Human neutrophils (5×10^5 cells/0.5 mL Hanks buffer) were preincubated with the indicated concentrations of 3G8 F(ab′)$_2$ or 10 μg/mL of irrelevant 320 F(ab′)$_2$ for 30 minutes at 37°C before cell activation with fLMF (10^{-6}M), and luminol-amplified chemiluminescence was measured. Blue and red curves represent 3G8 F(ab′)$_2$ anti-FcγRIII at 10 and 5 μg/mL, respectively, whereas black curves indicate the control 320 F(ab′)$_2$ at 10 μg/mL.

up to 6 hours) of SHP-1. Interestingly, in agreement with the delayed action of IVIg (Figure 5D), the kinetics of recruitment of these signaling effectors was also delayed after IVIg treatment compared with 3G8 F(ab′)$_2$. The recruitment of SHP-1 was accompanied by the concomitant phosphorylation of SHP-1. In *FcγRIIB*$^{-/-}$ BMMs the situation was slightly different in that both Syk and SHP-1 were already constitutively associated with endogenous FcγRIII in unstimulated cells (data not shown) as previously observed.[23] Again, preincubation with IVIg or 2.4G2 F(ab′)$_2$ enhanced recruitment of these effectors (data not shown). These experiments indicate that FcγRIII targeting induced an ITAMi configuration characterized by activation and recruitment of the negative signaling effector SHP-1. Furthermore, FcγRIII ITAMi configuration was able to block the IgE-dependent MAP-kinase pathway in transfectants that express the FcγRIII-FcRγ chimera, as demonstrated by inhibition of ERK phosphorylation after IVIg or 3G8 F(ab′)$_2$ treatment (supplemental Figure 7). Of note, IVIg and 3G8 F(ab′)$_2$ had no effect on the IgE-dependent Erk-signaling pathway in nontransfected RBL-2H3 cells indicating that this inhibition required relevant FcγRIII expression. To demonstrate the role of SHP-1 in mediating ITAMi signaling through mouse or human FcγRIII, we used either BMMs from SHP-1 deficient mice (*mev*/*mev*) or RBL-2H3 transfectants expressing FcγRIII-FcRγ chimera after specific knockdown of SHP-1. In both cases, IVIg failed to induce inhibition through FcγRIII in the absence of SHP-1 compared with controls (Figure 6B, supplemental Figure 8). As intracellular calcium mobilization is required for cell activation,[44] we next assessed whether the increase in intracellular calcium concentration ($[Ca^{2+}]_i$), was impaired by either 3G8 F(ab)$_2$ or IVIg treatment. FcεRI-mediated stimulation readily induced Ca^{2+} influx in Fura-2-AM–loaded FcγRIII-FcRγ transfectants. This response was markedly inhibited by preincubation with either 3G8 F(ab′)$_2$ or IVIg compared with irrelevant controls (Figure 6C). Of note, Ca^{2+} mobilization was more strongly inhibited by 3G8 than IVIg in agreement with strong inhibitory effect on endocytosis or phagocytosis. No inhibitory effect on Ca^{2+} entry was observed by either 3G8 F(ab′)$_2$ or IVIg in untransfected cells and in transfectants bearing ITAM-mutated forms (supplemental Figure 9), clearly indicating ITAM dependency of inhibitory responses. To discriminate between calcium release from intracellular stores and calcium entry from external medium, cells were treated with the calcium-chelating agent EGTA shortly before stimulation with antigen. Intracellular calcium mobilization under these conditions was strongly reduced by 3G8 F(ab′)$_2$ treatment (supplemental Figure 10). This inhibition was not observed in nontransfected cells, which show that inhibition mediated by FcγRIII was upstream to the calcium release from intracellular stores.

ITAMi signaling has been shown in the case of FcαRI to involve formation of polarized intracellular clusters named "inhibisomes," which enable ITAMi-recruited SHP-1 to target activating receptors independent of coligation at the cell surface.[22] We examined whether FcγRIII ITAMi signaling similarly induced intracellular coclustering with the targeted FcεRI. Confocal analysis showed that 3G8 F(ab′)$_2$ targeting of FcγRIII induced the codistribution of FcγRIII and FcεRI in intracellular clusters as typical inhibisomes (Figure 6D). As expected for such structures, the inhibitory SHP-1 phosphatase was colocalized with these receptors.

Relevance of FcγRIII inhibitory targeting in vivo by IVIg or anti-FcγRIII antibodies

To demonstrate the role of ITAMi-mediated FcγRIII-dependent inhibition in vivo, we chose to use IVIg in an antibody-independent

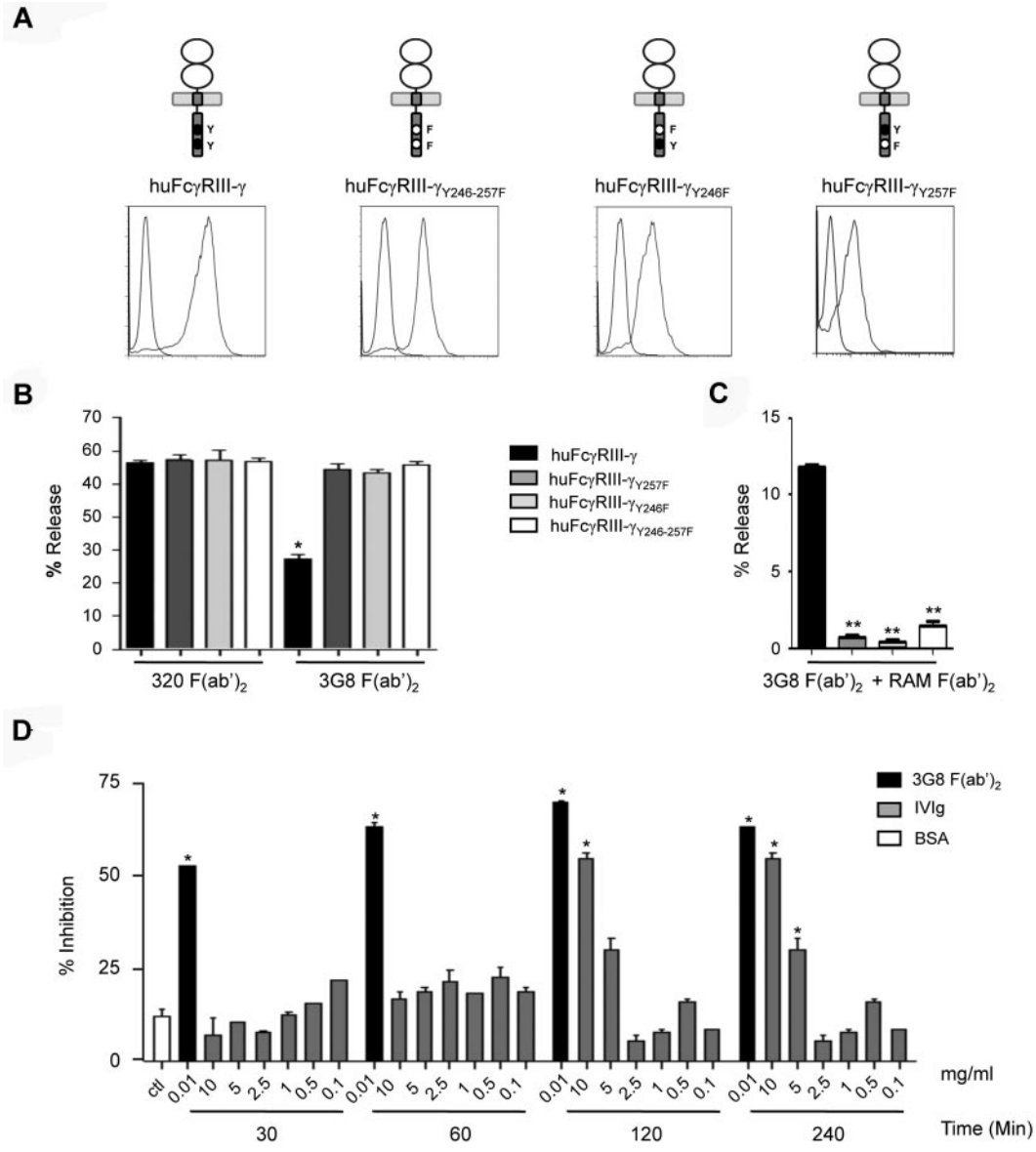

Figure 5. Human FcγRIIIA mediates both inhibition and activation through the FcRγ ITAM depending on the type of ligand. (A) FcγRIIIA chimeric constructs are schematically presented and their surface expression levels after transfection into RBL-2H3 cells are shown compared with nontransfected cells (gray vs blue histograms). (B) IgE-sensitized RBL-2H3 transfectants were incubated with either 3G8 F(ab′)$_2$ or 320 F(ab′)$_2$ at 10 μg/mL for 30 minutes at 37°C as indicated and degranulation was triggered with DNP-HSA (0.1 μg/mL) for 45 minutes. Net β-hexosaminidase release was determined. (*$P < .05$; n = 3; nonparametric Mann-Whitney test). (C) RBL-2H3 transfectants were incubated with 10 μg/mL of 3G8 F(ab′)$_2$ at 4°C before stimulation with rabbit anti–mouse F(ab′)$_2$ (RAM at 40 μg/mL) for 45 minutes at 37°C. Net β-hexosaminidase release was determined. (**$P < .01$; n = 3; nonparametric Mann-Whitney test). (D) IgE-sensitized huFcγRIII$^+$ RBL-2H3 transfectants were preincubated at 37°C with either BSA at 10 mg/mL for 240 minutes or 3G8 F(ab′)$_2$ or with IVIg, at the indicated concentrations and for the indicated time. Degranulation was measured as in panel B (*$P < .05$; n = 3, nonparametric Mann-Whitney test).

inflammatory model of obstructive nephropathy after UUO.[21,36] This strategy allowed to exclude competition effects of IVIg on FcγRs involved in models of IgG immune-complex–mediated autoimmune diseases.[1] Targeting FcγRIII ITAMi in UUO model also allowed to investigate whether heterologous receptors such as chemokine and cytokine receptors were inhibited as is the case for FcαRI.[21] We first analyzed the effect of 2.4G2 F(ab′)$_2$, which directly targeted FcγRIII in the background of FcγRIIB-deficiency, and induced similar to 3G8 (Figure 6), phosphorylation of SHP-1 in *FcγRIIB*$^{-/-}$ BMM (supplemental Figure 11). In vivo, treatment with 2.4G2 F(ab′)$_2$ markedly reduced inflammatory cell infiltrates in the obstructed kidney of Balb/c *FcγRIIB*$^{-/-}$ mice (Figure 7A). This anti-inflammatory effect was not observed in *FcγRIII*$^{-/-}$ mice (data not shown) indicating that FcγRIII mediates a major inhibitory function. Morever, IVIg treatment was also able to prevent macrophage infiltration to the obstructed kidney of Balb/c *FcγRIIB*$^{-/-}$ mice, and again this inhibition was not observed in the absence of FcγRIII (Figure 7A bottom panels).

Further examination of the proinflammatory response showed that expression levels of cytokine transcripts such as MCP-1 and TNFα in kidneys after UUO were also markedly down-regulated both after 2.4G2 F(ab′)$_2$ and IVIg treatment (Figure 7B). Again, this anti-inflammatory effect was not observed in *FcγRIII*$^{-/-}$ mice, which rule out inhibition through other FcRs in the absence of coligation (Figure 7B). Together, these results indicate that targeting of FcγRIII by either anti-FcγRIII F(ab′)$_2$ or IVIg has a remarkable anti-inflammatory effect by limiting proinflammatory

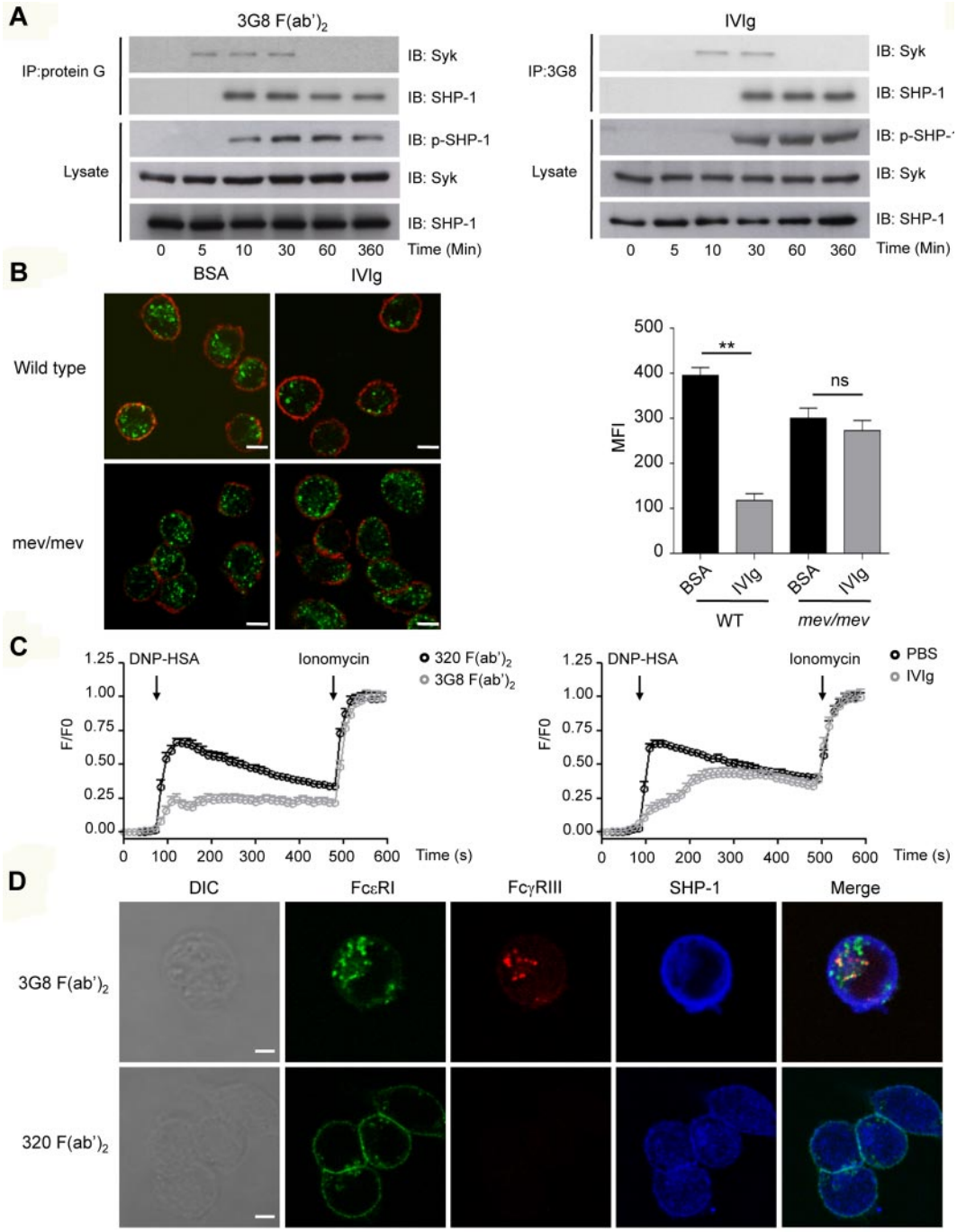

Figure 6. Monovalent and bivalent targeting of FcγRIII induce SHP-1 dependent ITAMi signaling and inhibisome formation. (A) huFcγRIII$^+$ RBL-2H3 transfectants were incubated with either 3G8 F(ab′)$_2$ (10 μg/mL) or IVIg (10 mg/mL) for the indicated times at 37°C. Cells were solubilized in 1% digitonin lysis buffer and immunoprecipitated with sepharose-coupled protein G sepharose (left panel) or with 3G8 F(ab′)$_2$ fragment coupled to CNBr-activated sepharose 4B (right panel), and then immunoblotted (IB) with anti-SHP1 or anti-Syk antibodies. Total lysates were analyzed for SHP-1 phosphorylation by immunoblotting with anti-phospho–SHP-1 (p-SHP1) antibody. The amounts of SHP-1 and Syk in lysates were analyzed in parallel using anti–SHP-1 or anti-Syk antibodies. (B) LPS-primed BMMs from WT and *mev/mev* mice were incubated with IVIg (18 mg/mL) or with BSA (18 mg/mL) for 30 minutes at 37°C. Alexa Fluor 488–coupled acLDL was added to allow endocytosis for 30 minutes followed by plasma membrane staining using anti-CD11b–biotin and streptavidin–Alexa 568 before confocal analyses. Left panels show representative merged optical sections of internalized acLDL inside the cell. Scale bars: 5 μm. Right panel indicates quantification of acLDL endocytosis using green MFI inside each cell as quantified by LSM510 analysis software that analyzes specific pixels in at least 5 confocal microscope fields (**$P < .01$; nonparametric Mann-Whitney test). Data are representative for at least 3 independent experiments. (C) IgE-sensitized huFcγRIII$^+$ RBL-2H3 transfectants were incubated with either 3G8 F(ab′)$_2$ (10 μg/mL) or IVIg (10 mg/mL) for 30 minutes at 37°C. Free intracellular Ca^{2+} was assessed after cell activation with DNP-HSA (0.1 μg/mL). After 7 minutes transfectants were stimulated with 1 μM ionomycin to determine maximal calcium uptake (n = 30 cells in each group). (D) Alexa 488–IgE sensitized huFcγRIII$^+$ RBL-2H3 transfectants were incubated for 30 minutes with etheir biotinylated 3G8 F(ab′)$_2$ or biotinylated 320 F(ab′)$_2$ at 10 μg/mL before addition of DNP-HSA antigen for 10 minutes. Cells were then fixed, permeabilized and further incubated with rabbit anti–SHP-1 antibodies followed by goat anti–rabbit Alexa Fluor 647. For detection of FcγRIII, Alexa Fluor 568–conjugated steptavidin was used. Receptors (FcεRI in green, FcγRIII in red) and SHP-1 (in blue) were analyzed by confocal microscopy. DIC and representative single optical sections through individual cells, as well as the merged images (xy planes), are presented. Scale bars: 5 μm. Data are representative of at least 3 independent experiments.

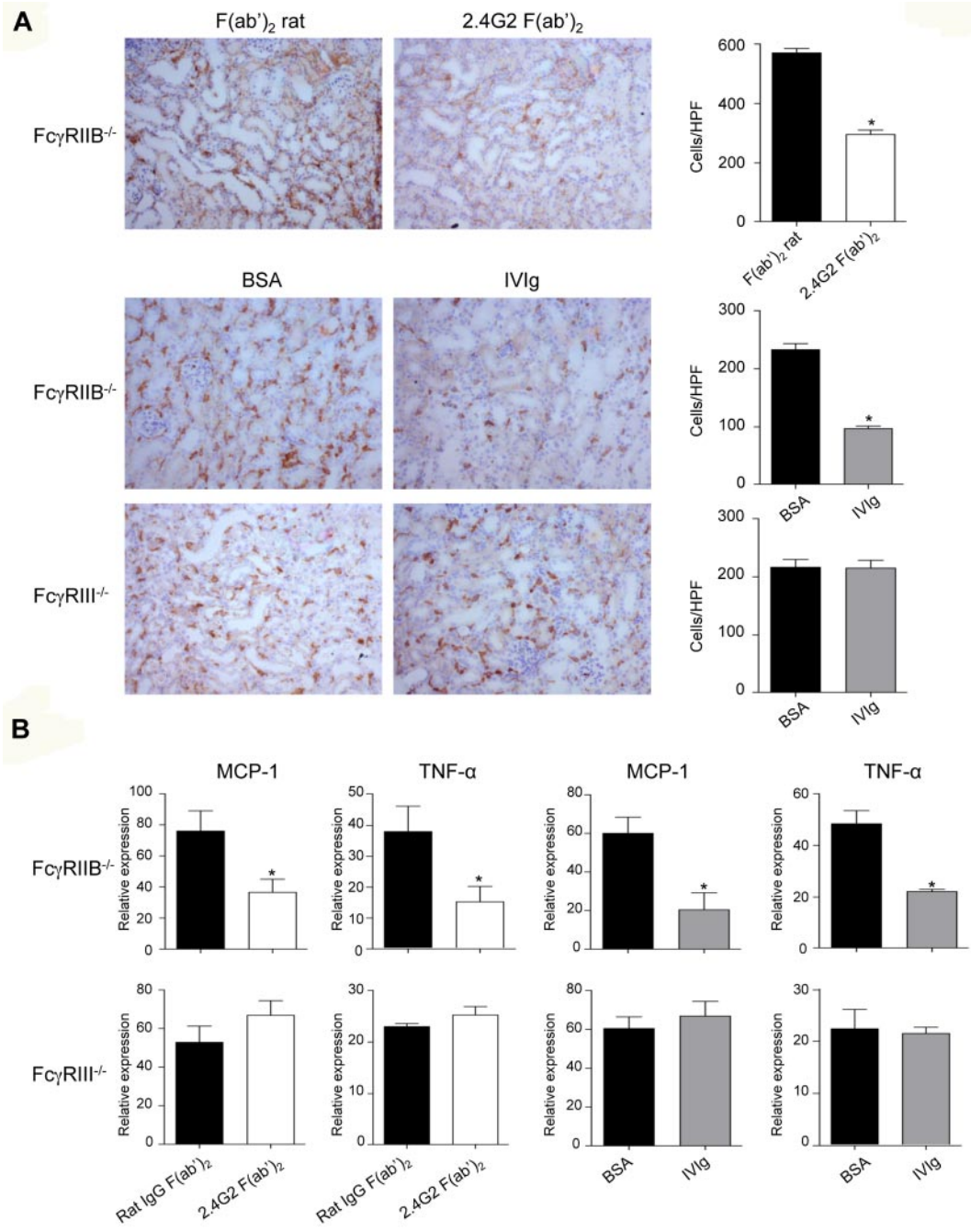

Figure 7. FcγRIII targeting by IVIg and 2.4G2 F(ab′)$_2$ reduces nonimmune inflammatory response in *FcγRIIB*$^{-/-}$ mice, but not in *FcγRIII*$^{-/-}$ mice. (A) *FcγRIIB*$^{-/-}$ or *FcγRIII*$^{-/-}$ Balb/c mice were injected intraperitonealy with 2.4G2 F(ab′)$_2$ (100 μg/20 g; top panel) or IVIg (40 mg/20 g; bottom panels), or their controls rat IgG F(ab′)$_2$ or BSA, respectively, as indicated. After 24 hours, mice were subjected to surgery for unilateral ureteral obstruction on their left side and 2.4G2 or IVIg or control treatments were continued at 48-hour intervals until day 8 when animals were killed and kidney sections were analyzed. Photographs show immunohistologic staining of CD11b-positive cells in obstructed left kidneys. Corresponding quantitative analysis of infiltrating cells of several animals (n = 6) is shown on the right. (*$P < .05$,**$P < .01$; nonparametric Mann-Whitney test). (B) Expression of MCP-1 and TNFα mRNA were analyzed by quantitative real-time PCR in obstructed kidney from mice treated with either IVIg or 2.4G2 F(ab′)$_2$ (white bar) or with their control treatment BSA or rat IgG F(ab′)$_2$ (black bar). Data represent relative mRNA expression levels of obstructed versus controlateral kidneys after normalization to GADPH (*$P < .05$; nonparametric Mann-Whitney test).

cytokines production in antibody-independent obstructive kidney inflammatory disease.

Discussion

At present, IgG isotypes have been considered as major actors in adaptive immune responses by their capacity to eliminate antigens through their combined interaction with antigen and either complement or multiple FcγRs.[45] Effector mechanisms depend on antigen recognition and formation of immune complexes. However, even in the absence of specific antigen at the concentrations present in serum, IgGs continuously interact with their corresponding receptors through the Fc domains. In the past, these interactions have been considered as without biologic consequences. Here, we provide clear evidence that the interaction of IgG with FcγRIII,

independently of antigen, can induce cell signaling through the ITAM with an overall inhibitory function toward a variety of heterologous activating receptors in the absence of coaggregation. Monomeric or dimeric targeting of mouse FcγRIII by either mouse IgG1, human IVIg, or anti-FcγRIII $F(ab')_2$ reduced MARCO-dependent acLDL endocytosis in primary macrophages. Recent evidence showed that *E coli* binding to mouse FcγRIII in an IgG-independent manner induces ITAMi signaling through this receptor that blocks MARCO-mediated phagocytosis thereby favoring immune evasion of the bacteria.[23] The present data suggest an opportunistic use of a physiologic inhibitory mechanism by *E coli*. More importantly, they also support the notion that FcγRIII mediates a dual activating and inhibitory function depending on the degree of aggregation of its natural ligand IgG. This inhibitory action of FcγRIII was not restricted to phagocytosis but affected also inflammatory mediator release. Indeed, IVIg or anti–human FcγRIII $F(ab')_2$ inhibited IgE-mediated exocytosis in RBL-2H3 cells transfected with human FcγRIII-FcRγ chimera as well as fMLF-mediated ROS production from isolated human blood monocytes. The observation that GPI-anchored FcγRIIIB on human neutrophils failed to mediate such functions was a strong indication of FcRγ involvement. This was further demonstrated by experiments using human FcγRIII-FcRγ fusion proteins. Analysis of the signaling mechanism using these transfectants clearly revealed an ITAMi configuration, similar to what has been observed for FcαRI by IgA and for FcγRIII by *E coli*.[20,23] ITAM involvement was demonstrated by analysis of tyrosine point mutations of the ITAM associated with the receptor chimeras as either of the 2 tyrosines was found necessary to generate the suppressive signal. Furthermore, as for FcαRI, both Syk and SHP-1 were recruited under inhibitory conditions. Kinetic analysis revealed 2 consecutive phases involved in inhibitory ITAMi signaling as previously predicted[46]: a preactivating phase characterized by the early and transient recruitment of Syk followed by stable recruitment of the inhibitory effector, SHP-1, which coincided with the appearance of the inhibitory action. The abolishment of inhibition in single Y-to-F FcRγ-ITAM mutant transfectants indicate that both tyrosine residues are required to SHP-1 recruitment to FcγRIII, which is in agreement with a previous observation that SHP-1 binding to inhibitory natural killer (NK) receptors requires tyrosine phosphorylation in 2 ITIM sequences.[47] This was observed for both anti-FcγRIII $F(ab')_2$ and IVIg ligands. SHP-1 recruitment also coincided with its phosphorylation on tyrosine 536 known to enhance its activity.[48] Kinetics of effector recruitment and SHP-1 phosphorylation was delayed after IVIg treatment compared with anti-FcγRIII antibody, in agreement with the lower affinity of IgG ligand for FcγRIII. SHP-1 is a major inhibitory effector of this ITAMi signaling as specific knockdown of this phosphatase reversed the inhibitory effect. In agreement with SHP-1 dependent action, we found a strong inhibition of the IgE-mediated Erk phosphorylation and calcium mobilization. Release of intracellular calcium stores was blocked by FcγRIII targeting indicating that the inhibitory receptor pathway initiated by ITAMi could affect multiple heterologous receptor signal transduction that rely on cytosolic calcium increases. In agreement with a local action, we identified inhibitory and activating receptors colocalized in intracellular structures previously defined as inhibisomes,[22] which enable local negative regulation by SHP-1 in absence of receptor coligation at the cell surface. These findings confirm inhibisomes as relevant cellular structures of ITAMi signaling. Interestingly, SHP-1 recruitment and phosphorylation is only observed after stimulation in RBL transfectants expressing human FcγRIII-γ chimera. This differs from what is observed in mouse cells expressing endogenous FcγRIII. Indeed, our previous data showed that mouse FcγRIII expressed by macrophages is constitutively in an ITAMi configuration through constitutive phosphorylation of associated FcRγ and recruitment of SHP-1 and syk[23] by a mechanism still unknown that may involve a yet unidentified cis-acting self-ligand. Still, targeting of FcγRIII with *E coli* increases this ITAMi configuration.[23] Independent of these considerations, constitutive phosphorylation and association of SHP-1 is not sufficient for inhibisome formation as this requires a second event provided by the stimulation of activating receptor and their engagement in rafts domain.[22] The inhibitory action was optimal at high concentrations of IgG (~10 mg/mL that is in the 10^{-4}-10^{-5}M range) that coincide with IgG concentrations found in serum in humans, which supports that this may be relevant in vivo. This is also in agreement with the fact that monomeric IgG1 binds FcγRIII through a low-affinity interaction with a $k_D > 10^{-6}$M.[49] It should be noted that IVIg consists of at least 90% intact IgG, with inhibitory IgG1 being the major component in IVIG preparations.[2,5] Furthermore, the therapeutic doses used in the treatment of autoimmune and inflammatory diseases (in the range of 400 mg/kg/d)[5] will increase IgG1 plasma levels, therefore shifting the balance toward an inhibitory mode of FcγRIIIA, as observed in our dose-response experiments. The fact that IgG dimers that also present in IVIg preparations or anti-FcγRIII $F(ab')_2$, but not multimers, induced such inhibitory signals is in support of the requirement of either monovalent or divalent interaction with FcγRIII. In this context, it is interesting to note that bivalent interaction with $F(ab)'_2$ antibodies showed a more rapid kinetics to reach inhibition compared with monomeric IgG, possibly because of the higher affinity of FcγRIII-specific antibodies. Strikingly, and in contrast to what has been observed for FcαRI,[20] anti-FcγRIII 3G8 Fab were ineffective in inducing inhibition. However, it should be noted that 1 of 4 anti-FcαRI Fab tested were unable to induce inhibition,[20] which suggests that conformational changes induced by some, but not all, specific antibodies may be important in the FcαRI inhibitory system. Whether such conformational changes are actually induced in FcαRI and FcγRIII by their respective monomeric ligands remain to be determined.

IVIgs are currently used for treatment of inflammatory and autoimmune diseases. Several mechanisms have been proposed for IVIg action, including ITIM-mediated FcγRIIB inhibitory signals[1,2] or involving DC-SIGN for a minor population of IgG.[6] A role for FcγRIII in IVIg-mediated inhibition has been reported in 2 studies[14,15] implicating activation of FcγRIII by large IgG immune complexes. Although Park-Min et al found that FcγRIII activation leads to the suppression of IFN-γ signaling by down-regulating expression of the IFNGR2 subunit of the IFN-γ receptor,[15] Siragam et al showed priming of regulatory activity by dendritic cells as the responsible mechanism.[14] Regulatory iNKT cells may also mediate IVIg-induced anti-inflammatory actions.[16] However, the implication of FcγRIII ITAMi in this inhibition has not been investigated. Both IVIg and 2.4G2 anti-FcγRII/III $F(ab')_2$ treatments were beneficial to prevent inflammation by reducing tissue macrophage infiltration and inflammatory mediator production in an inflammatory model of obstructed kidney in *FcγRIIB*$^{-/-}$ mice. This reduction was observed in the background of FcγRIIB deficiency, but completely absent in the FcγRIII deficiency, clearly establishing the importance of FcγRIII targeting. These in vivo data further confirm the capacity of ITAMi signaling to inhibit a wide array of heterologous receptors. This efficient prevention of an IgG-independent inflammatory reaction in vivo by targeting

FcγRIII establishes a rationale for a new line of therapeutic strategies with a wide range of applications. In addition, the more rapid inhibition observed after anti-FcγRIII $F(ab')_2$ treatment than after IVIg treatment opens the possibility for an alternative approach to IVIg than remains to be fully evaluated. Thus, our data point out a new mechanism of IVIg action, which involves ITAMi signaling via FcγRIII.

In summary, our conclusion that IVIg and IgG1 control inflammatory response by ITAMi signaling through FcγRIII is based on the following evidences: (1) in vitro targeting of FcγRIII with irrelevant IgG1 through its Fc portion inhibited endocytosis in a dose-dependent manner that reflects the IgG concentration found in serum; (2) in vitro targeting of FcγRIII with $F(ab')_2$ fragments of specific antibodies had the same effect as IgG, whether in mouse or in human cells, whereas targeting FcγRII did not although it has the same extracellular domain as FcγRIII; (3) in vitro targeting of FcγRIII with IVIg had the same effect as its targeting with irrelevant mouse IgG1 or with specific antibodies; (4) although we cannot exclude existence of natural antibodies directed against mouse FcγRIII in the human IVIg preparations used in our in vivo experiments, natural IgG antibodies have affinities to antigens that are in the same range as that of Fc domains of IgG for binding to FcγRIII[50]; thus, in vitro and in vivo engagement of FcγRIII by irrelevant IgG (through their Fc domain) or by natural antibodies present in IVIg preparations would promote tonic inhibitory signals of the same intensity; (5) in vivo targeting of FcγRIII (but not FcγRII) with $F(ab')_2$ fragments of specific antibodies was as efficient in preventing inflammation in the UUO model as IVIg acting through FcγRIII; and (6) the FcγRIII-mediated inhibitory signaling had all the biochemical hallmarks of an ITAMi signaling. We conclude that targeting FcγRIII in vivo either with IVIg (whether by natural antibodies present in the preparations or by Fc binding) or with an $F(ab')_2$ fragment of specific antibodies may have therapeutic relevance. However, it should be stressed that FcγRIII targeting is not the only means of action of IVIg because others have convincingly reported other ways of action for these immunoglobulins.[1,3-6] Thus, although VIg may use multiple and nonexclusive modes of action, FcγRIII targeting is one of these modes that could have potent therapeutic development.

Evolution might have designed multiple ways (both positive and negative) of controlling activation of the immune system. This system has powerfully destructive potential that needs to be properly kept in check for adapted immune responses. Thus, in the absence of antigen the immune system may not be dormant but constantly under control through interaction of large numbers of monomeric immunoglobulins with their cognate receptors. Introduction of antigens would shift this situation through multimeric interaction of immune complexes with FcγRIII that would both induce activating signals and weaken the inhibitory signals through a decrease in available FcγRIII for monomeric IgG binding. In this setting, ITIM signaling (through coaggregation of FcγRIIB and FcγRIII by immune complexes) would relay in part ITAMi signaling for inhibition; this relay growing in intensity when the ITAMi signal would weaken after raising levels of circulating immune complexes. Altogether, our data support a new paradigm of immune homeostasis regulation by monomeric IgG.

Acknowledgments

The authors thank Samira Benadda for confocal analyses, Nathalie Ialy-Radio and Anissa Bouhalfaïa for animal care, and Jamel El Benna for chemiluminescence analysis.

This work was supported in part by grants from Agence National de la Recherche (ANR) MIE 2009. S.B.M. was a recipient from Association pour la Recherche contre le Cancer. M.A. was supported by Fondation pour la Recherche Médicale.

Authorship

Contribution: M.A. conducted major experiments and wrote the paper; S.B.M. performed signalling studies; M.B.-P. generated transfectants; T.B. conducted ROS analysis; H.S. performed calcium influx studies; E.R. helped with degranulation experiments; M.B. provided scientific discussion and critical reading of the paper; B.C. provided human cell samples; Z.Z. provided cells from the homozygous viable motheaten mice; U.B. provided critical scientific discussion and wrote the paper; P.L. designed calcium experiments, analyzed data and wrote the paper; and R.C.M. designed the study, analyzed data, and wrote the paper.

Conflict-of-interest disclosure: The authors declare no competing financial interests.

Correspondence: Renato C. Monteiro, Inserm U699, Paris, F-75018, France and Université Paris Diderot, Sorbonne Paris Cité, Faculté de Médecine, Site Xavier Bichat, Paris, F-75018, France; e-mail: renato.monteiro@inserm.fr.

References

1. Nimmerjahn F, Ravetch JV. Anti-inflammatory actions of intravenous immunoglobulin. *Annu Rev Immunol*. 2008;26:513-533.
2. Tha-In T, Bayry J, Metselaar HJ, Kaveri SV, Kwekkeboom J. Modulation of the cellular immune system by intravenous immunoglobulin. *Trends Immunol*. 2008;29(12):608-615.
3. Crow AR, Song S, Siragam V, Lazarus AH. Mechanisms of action of intravenous immunoglobulin in the treatment of immune thrombocytopenia. *Pediatr Blood Cancer.* 2006;47(5 suppl): 710-713.
4. Bussel JB. Another interaction of the FcR system with IVIG. *Thromb Haemost.* 2002;88(6):890-891.
5. Negi VS, Elluru S, Siberil S, et al. Intravenous immunoglobulin: an update on the clinical use and mechanisms of action. *J Clin Immunol.* 2007; 27(3):233-245.
6. Anthony RM, Kobayashi T, Wermeling F, Ravetch JV. Intravenous gammaglobulin suppresses inflammation through a novel T(H)2 pathway. *Nature.* 2011; 475(7354):110-113.
7. Nimmerjahn F, Ravetch JV. Fcgamma receptors as regulators of immune responses. *Nat Rev Immunol.* 2008;8(1):34-47.
8. Wang AV, Scholl PR, Geha RS. Physical and functional association of the high affinity immunoglobulin G receptor (Fc gamma RI) with the kinases Hck and Lyn. *J Exp Med.* 1994;180(3): 1165-1170.
9. Ghazizadeh S, Bolen JB, Fleit HB. Physical and functional association of Src-related protein tyrosine kinases with Fc gamma RII in monocytic THP-1 cells. *J Biol Chem.* 1994;269(12):8878-8884.
10. Hazenbos WL, Gessner JE, Hofhuis FM, et al. Impaired IgG-dependent anaphylaxis and Arthus reaction in Fc gamma RIII (CD16) deficient mice. *Immunity.* 1996;5(2):181-188.
11. Meyer D, Schiller C, Westermann J, et al. FcgammaRIII (CD16)-deficient mice show IgG isotype-dependent protection to experimental autoimmune hemolytic anemia. *Blood.* 1998;92(11): 3997-4002.
12. Nimmerjahn F, Ravetch JV. Divergent immunoglobulin g subclass activity through selective Fc receptor binding. *Science.* 2005;310(5753):1510-1512.
13. Vivier E, Daeron M. Immunoreceptor tyrosine-based inhibition motifs. *Immunol Today.* 1997; 18(6):286-291.
14. Siragam V, Crow AR, Brinc D, Song S, Freedman J, Lazarus AH. Intravenous immunoglobulin ameliorates ITP via activating Fc gamma receptors on dendritic cells. *Nat Med.* 2006;12(6):688-692.
15. Park-Min KH, Serbina NV, Yang W, et al. FcgammaRIII-dependent inhibition of interferon-gamma responses mediates suppressive effects of intravenous immune globulin. *Immunity.* 2007; 26(1):67-78.

16. Araujo LM, Chauvineau A, Zhu R, et al. Cutting edge: intravenous Ig inhibits invariant NKT cell-mediated allergic airway inflammation through FcgammaRIIIA-dependent mechanisms. *J Immunol.* 2011;186(6):3289-3293.
17. Hamerman JA, Lanier LL. Inhibition of immune responses by ITAM-bearing receptors. *Sci STKE.* 2006;2006(320):re1.
18. Blank U, Launay P, Benhamou M, Monteiro RC. Inhibitory ITAMs as novel regulators of immunity. *Immunol Rev.* 2009;232(1):59-71.
19. Ivashkiv LB. Cross-regulation of signaling by ITAM-associated receptors. *Nat Immunol.* 2009; 10(4):340-347.
20. Pasquier B, Launay P, Kanamaru Y, et al. Identification of FcalphaRI as an inhibitory receptor that controls inflammation: dual role of FcRgamma ITAM. *Immunity.* 2005;22(1):31-42.
21. Kanamaru Y, Pfirsch S, Aloulou M, et al. Inhibitory ITAM signaling by Fc alpha RI-FcR gamma chain controls multiple activating responses and prevents renal inflammation. *J Immunol.* 2008; 180(4):2669-2678.
22. Pfirsch-Maisonnas S, Aloulou M, Xu T, et al. Inhibitory ITAM signaling traps activating receptors with the phosphatase SHP-1 to form polarized "inhibisome" clusters. *Sci Signal.* 2011;4(169): ra24.
23. Pinheiro da Silva F, Aloulou M, Skurnik D, et al. CD16 promotes Escherichia coli sepsis through an FcR gamma inhibitory pathway that prevents phagocytosis and facilitates inflammation. *Nat Med.* 2007;13(11):1368-1374.
24. Takai T, Ono M, Hikida M, Ohmori H, Ravetch JV. Augmented humoral and anaphylactic responses in Fc gamma RII-deficient mice. *Nature.* 1996; 379(6563):346-349.
25. Takai T, Li M, Sylvestre D, Clynes R, Ravetch JV. FcR gamma chain deletion results in pleiotrophic effector cell defects. *Cell.* 1994;76(3):519-529.
26. Zhang L, Oh SY, Wu X, et al. SHP-1 deficient mast cells are hyperresponsive to stimulation and critical in initiating allergic inflammation in the lung. *J Immunol.* 2010;184(3):1180-1190.
27. Shultz LD, Schweitzer PA, Rajan TV, et al. Mutations at the murine motheaten locus are within the hematopoietic cell protein-tyrosine phosphatase (Hcph) gene. *Cell.* 1993;73(7):1445-1454.
28. Nishiya T, DeFranco AL. Ligand-regulated chimeric receptor approach reveals distinctive subcellular localization and signaling properties of the Toll-like receptors. *J Biol Chem.* 2004;279(18): 19008-19017.
29. Unkeless JC. Characterization of a monoclonal antibody directed against mouse macrophage and lymphocyte Fc receptors. *J Exp Med.* 1979; 150(3):580-596.
30. Fleit HB, Wright SD, Unkeless JC. Human neutrophil Fc gamma receptor distribution and structure. *Proc Natl Acad Sci U S A.* 1982;79(10):3275-3279.
31. Silvain C, Patry C, Launay P, Lehuen A, Monteiro RC. Altered expression of monocyte IgA Fc receptors is associated with defective endocytosis in patients with alcoholic cirrhosis. Potential role for IFN-gamma. *J Immunol.* 1995;155(3):1606-1618.
32. Liu FT, Bohn JW, Ferry EL, et al. Monoclonal dinitrophenyl-specific murine IgE antibody: preparation, isolation, and characterization. *J Immunol.* 1980;124(6):2728-2737.
33. Monteiro RC, Cooper MD, Kubagawa H. Molecular heterogeneity of Fc alpha receptors detected by receptor-specific monoclonal antibodies. *J Immunol.* 1992;148(6):1764-1770.
34. van der Laan LJ, Dopp EA, Haworth R, et al. Regulation and functional involvement of macrophage scavenger receptor MARCO in clearance of bacteria in vivo. *J Immunol.* 1999;162(2):939-947.
35. Roa M, Paumet F, Le Mao J, David B, Blank U. Involvement of the ras-like GTPase rab3d in RBL-2H3 mast cell exocytosis following stimulation via high affinity IgE receptors (Fc epsilonRI). *J Immunol.* 1997;159(6):2815-2823.
36. Inazaki K, Kanamaru Y, Kojima Y, et al. Smad3 deficiency attenuates renal fibrosis, inflammation, and apoptosis after unilateral ureteral obstruction. *Kidney Int.* 2004;66(2):597-604.
37. Kanamaru Y, Arcos-Fajardo M, Moura IC, et al. Fc alpha receptor I activation induces leukocyte recruitment and promotes aggravation of glomerulonephritis through the FcR gamma adaptor. *Eur J Immunol.* 2007;37(4):1116-1128.
38. Bowdish DM, Gordon S. Conserved domains of the class A scavenger receptors: evolution and function. *Immunol Rev.* 2009;227(1):19-31.
39. Fournier EM, Siberil S, Costes A, et al. Activation of human peripheral IgM+ B cells is transiently inhibited by BCR-independent aggregation of Fc gammaRIIB. *J Immunol.* 2008;181(8):5350-5359.
40. Clynes R. Protective mechanisms of IVIG. *Curr Opin Immunol.* 2007;19(6):646-651.
41. Nimmerjahn F, Ravetch JV. Fcgamma receptors: old friends and new family members. *Immunity.* 2006;24(1):19-28.
42. Doerner AM, Chen LY, Ye RD, Yong J, Huang S, Pan ZK. Cell type-specific release of matrix-metallo-proteinase-9 by bacterial chemoattractant in human blood phagocytic leukocytes. *Int J Clin Exp Med.* 2011;4(1):67-73.
43. Boussetta T, Gougerot-Pocidalo MA, Hayem G, et al. The prolyl isomerase Pin1 acts as a novel molecular switch for TNF-alpha-induced priming of the NADPH oxidase in human neutrophils. *Blood.* 2010;116(26):5795-5802.
44. Mohr FC, Fewtrell C. IgE receptor-mediated depolarization of rat basophilic leukemia cells measured with the fluorescent probe bis-oxonol. *J Immunol.* 1987;138(5):1564-1570.
45. Woof JM, Burton DR. Human antibody-Fc receptor interactions illuminated by crystal structures. *Nat Rev Immunol.* 2004;4(2):89-99.
46. Pinheiro da Silva F, Aloulou M, Benhamou M, Monteiro RC. Inhibitory ITAMs: a matter of life and death. *Trends Immunol.* 2008;29(8):366-373.
47. Long EO. Negative signaling by inhibitory receptors: the NK cell paradigm. *Immunol Rev.* 2008; 224:70-84.
48. Zhang Z, Shen K, Lu W, Cole PA. The role of C-terminal tyrosine phosphorylation in the regulation of SHP-1 explored via expressed protein ligation. *J Biol Chem.* 2003;278(7):4668-4674.
49. Bruhns P, Iannascoli B, England P, et al. Specificity and affinity of human Fcgamma receptors and their polymorphic variants for human IgG subclasses. *Blood.* 2009;113(16):3716-3725.
50. Spalter SH, Kaveri SV, Bonnin E, Mani JC, Cartron JP, Kazatchkine MD. Normal human serum contains natural antibodies reactive with autologous ABO blood group antigens. *Blood.* 1999; 93(12):4418-4424.